JOURNAL OF SOLID STATE CHEMISTRY 110, 226–233 (1994)

Synthesis and Crystal Structure of a New Mixed Orthovanadate–Pyrovanadate Series: $M Ba_2V_3O_{11}$ or $M Ba_2V_2PO_{11}$ with M = Bi, In, or a Rare Earth

Jinfan Huang, Qiuyi Gu, and Arthur W. Sleight

Department of Chemistry, Oregon State University, Corvallis, Oregon 97331-4003

Received September 14, 1992; in revised form September 8, 1993; accepted September 17, 1993

A new series of vanadates with the general formula $M Ba_2V_3O_{11}$, where M may be Bi, In, or a rare earth, has been synthesized and structurally characterized by single crystal X-ray diffraction and powder X-ray diffraction. The general formula may be rewritten as $M Ba_2(VO_4)(V_2O_7)$ to emphasize that there is one orthovanadate group and one pyrovanadate group in each formula unit. Up to one-third of the vanadium may be replaced by phosphorous, leading to the general formula $M Ba_2V_2PO_{11}$. However, phosphorous shows no preference between the ortho and pyro groups. Both $M Ba_2V_3O_{11}$ and $M Ba_2V_2PO_{11}$ crystallize in the monoclinic system with the space group $P2_1/c$ and $Z = 4$. The cell parameters from single crystal X-ray data of $BiBa_2V_3O_{11}$ are $a = 12.332(4)$ Å, $b = 7.750(4)$ Å, $c = 11.279(4)$ Å, $\beta = 103.22(3)°$, $V = 1049(1)$ Å^3; and for $BiBa_2V_2PO_{11}$ are $a = 12.266(2)$ Å, $b = 7.615(2)$ Å, $c = 11.312(2)$ Å, $\beta = 103.32(2)°$, $V = 1028.2(2)$ Å^3. The Bi atom coordinates to six oxygen atoms forming a distorted octahedron, and the edge sharing of BiO_6 octahedra results in a BiO_4 chain along the b axis. There are two types of Ba atoms with coordination numbers of 10 and 11. There are three types of tetrahedral (T) atoms in these structures. The nonequivalent T atoms of the pyro group give T–O–T angles of 167 and 171° in $BiBa_2V_3O_{11}$ and $BiBa_2V_2PO_{11}$, respectively. Isostructural $M Ba_2V_3O_{11}$ compounds were prepared in which M is In, La, Ce, Pr, Nd, Sm, Eu, Gd, Tb, Dy, Ho, Er, Yb, or Lu.

INTRODUCTION

In a recent paper (1), we reported a new bismuth strontium vanadate, $BiSr_2V_3O_{11}$, that contains both an orthovanadate group $(VO_4)^{3-}$ and a pyrovanadate group $(V_2O_7)^{4-}$. In that paper, we indicated that the substitution of Sr for Ba resulted in a different structure type which still contains both the orthovanadate and the pyrovanadate groups. In this paper, we describe the synthesis and the crystal structure of $M Ba_2V_3O_{11}$ and $M Ba_2V_2PO_{11}$ where M = Bi, In, or a rare earth.

EXPERIMENTAL

The powder samples of the title compounds were prepared by solid state reactions. The reagents used were Bi_2O_3 (J. T. Baker, Inc., 99.6%), In_2O_3 (J. T. Baker Inc., 99.99%), $Sc_2(C_2O_4) \cdot 5H_2O$ (Johnson Matthey, 99.99%), Y_2O_3 (Johnson Matthey, 99.9%), $BaCO_3$ (J. T. Baker Inc., 99.9%), NH_4VO_3 (J. T. Baker Inc., 99.1%) or V_2O_5 (Johnson Matthey Electronics, 99.9%), and reagent $(NH_4)_2HPO_4$ (E. M. Science). Combined differential thermal analysis (DTA) and thermal gravity analysis (TGA) at a heating rate of 10°C/min was first performed on each stoichiometric mixture of the reagents to determine the appropriate reaction conditions for synthesis. For the mixture $1/2Bi_2O_3 + 2BaCO_3 + 3NH_4VO_3$, the decomposition of NH_4VO_3 starts at 200°C and completes at about 450°C. Reaction to form $BiBa_2V_3O_{11}$ apparently starts at about 620°C and is completed by about 780°C. This product melts congruently at 1045°C. For the mixture of $1/2Bi_2O_3 + 2BaCO_3 + V_2O_5 + (NH_4)_2HPO_4$, the decomposition of $(NH_4)_2HPO_4$ starts at 160°C and completes at about 380°C; the reaction to product starts at about 500°C and ends at 720°C. The product $BiBa_2V_2PO_{11}$ melts at about 980°C. The reaction temperature to form the $R Ba_2V_3O_{11}$ rare earth compounds is lower; however, these products melt incongruently at higher temperatures. For example, $EuBa_2V_3O_{11}$ melts at about 1260°C. Based on the thermal analysis, all the mixtures were first heated at 450°C for 4 hr to decompose NH_4VO_3 or $(NH_4)_2HPO_4$. After regrinding of the mixtures, they were heated at 700°C for 12 hr and 850°C for 24 hr in air.

The X-ray powder diffraction patterns of all the samples were obtained using a Siemens D5000 diffractometer with CuK_α radiation and silicon as an internal standard. The results from the X-ray powder diffraction patterns indicate the formation of a new family of compounds with formulas $M Ba_2V_3O_{11}$ and $M Ba_2V_2PO_{11}$, where M may be Bi, In, or rare earth.

0022-4596/94 $6.00

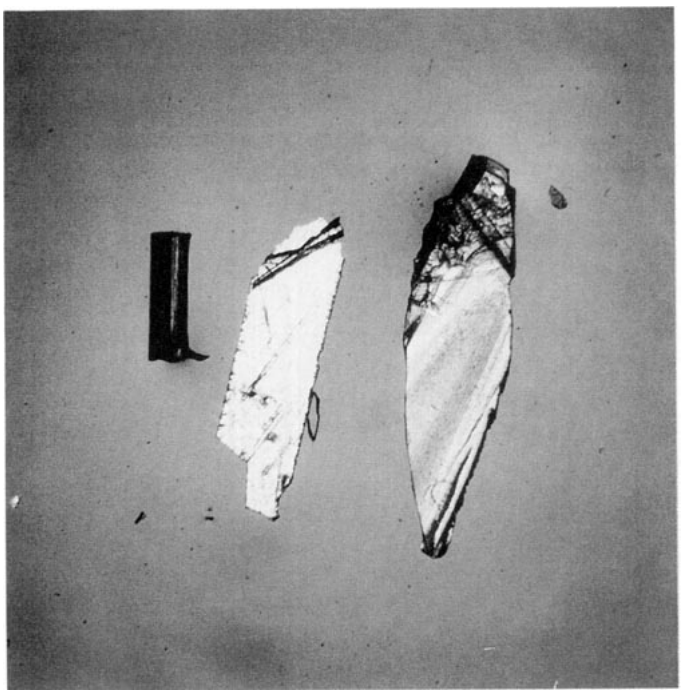

FIG. 1. Crystals of $MBa_2T_3O_{11}$ compounds. From left to right are (1) brick crystal of $BiBa_2V_2PO_{11}$; (2) flat crystal of $EuBa_2V_3O_{11}$; (3) flat crystal of $BiBa_2V_3O_{11}$.

To grow single crystals, the aforementioned powder samples were melted at temperatures 30°C above their melting points. After being held at this temperature for 10 min, the samples were cooled to 600°C at the rate of 15°C/hr and then cooled to room temperature by simply turning off the power to the furnace. Thin flat crystals were usually obtained for $MBa_2V_3O_{11}$ compounds, and long brick-shaped crystals were obtained for $BiBa_2V_2PO_{11}$. Figure 1 shows the flat morphology of $BiBa_2V_3O_{11}$ and $EuBa_2V_3O_{11}$ crystals, and the brick morphology of a $BiBa_2V_2PO_{11}$ crystal. Single crystals were analyzed with an SX-50 electron microprobe using Bi_2O_3, rare earth containing Ca–Al–Si–O glasses, $BaTiSi_3O_9$, $Pb_5Cl(VO_4)_3$, and $Ca_5(PO_4)_3(F_{0.5}Cl_{0.5})$ as standards for Bi, rare earths, Ba, V, and P, respectively. The averaged results indicated the composition of the title compounds.

Crystals of $BiBa_2V_2PO_{11}$ and $BiBa_2V_3O_{11}$ were mounted on glass fibers for data collection. Details of the data collection, reduction, and the refinement are summarized in Table 1. The lattice constants were determined by a least-squares analysis of 25 reflections that had been centered on a Rigaku AFC6R diffractometer in the range of $25.5° < 2\theta < 29.7°$ for $BiBa_2V_2PO_{11}$ and 20 reflections in the range of $28.8° < 2\theta < 43.1°$ for $BiBa_2V_3O_{11}$. The data were collected with the $\omega - 2\theta$ scan technique at a scan width $\Delta\omega = (1.63 + 0.3 \tan\theta)°$ for $BiBa_2V_2PO_{11}$ and $\Delta\omega = (1.30 + 0.3 \tan\theta)°$ for $BiBa_2V_3O_{11}$. The intensities of three standard reflections measured every 300 reflections throughout data collection exhibited no significant fluctuations.

The crystal structure of $BiBa_2V_2PO_{11}$ was solved and refined with the programs from TEXSAN crystallographic software package (2). The positions of the atoms Bi, Ba, and V in $BiBa_2V_2PO_{11}$ were determined from direct methods SHELXS (3). The oxygen atoms were located from subsequent analyses of difference electron density maps. No peaks were found for P atoms and the relative shorter V–O distances in the Fourier map indicates some P on the "V sites." For $BiBa_2V_2PO_{11}$ crystals grown with excess phosphorous, microprobe analysis showed a V-to-P ratio of 2.0 within the error of determination. Furthermore, refinement of occupancy parame-

TABLE 1
Crystal Data and Intensity Collection for $BiBa_2V_2PO_{11}$ and $BiBa_2V_3O_{11}$

	$BiBa_2V_2PO_{11}$	$BiBa_2V_3O_{11}$
Color	Light yellow	Light yellow
Size (mm)	0.1 × 0.1 × 0.2	0.1 × 0.1 × 0.1
Crystal system	Monoclinic	Monoclinic
Space group	$P2_1/c$ (No. 14)	$P2_1/c$ (No. 14)
a (Å)	12.266(2)	12.332(4)
b (Å)	7.615(2)	7.750(4)
c (Å)	11.312(2)	11.279(6)
β (°)	103.32(2)	103.22(3)
Volume (Å^3)	1028.2(4)	1049(1)
Z	4	4
Formula weight	792.49	812.46
Calculated Density (g/cm^3)	5.119	5.142
Diffractometer	Rigaku AFC6R	
Radiation	Mo$K\alpha$ (λ = 0.71069 Å) Graphite-monochromated	
Temperature	23°C	
ν (Mo) (cm^{-1})	264.62	265.8
Maximum $2q$(°)	70.0	70.0
Data collected	$0 < h < 18$	$0 < h < 18$
	$0 < k < 12$	$-12 < k < 12$
	$-20 < l < 20$	$-20 < l < 20$
Scan method	$\omega - 2\theta$	
Scan speed (deg/min)	16.0 in ω, and 32 in 2θ	
No. of data collected	3428	4703
No. unique data	3251	2450
R_{int}	0.072	0.089
No. observations with $F_0^2 > 3\sigma(F_0^2)$	2201	1421
Parameters varied	155	69
Data/parameter ratio	14.20	20.59
Absorption correction	DIFABS	
Transmission factors, range	0.86–1.22	0.85–1.11
Refinement method	Full-matrix least-squares on $\|F\|$	
Weight scheme		
R	0.055	0.042
R_w	0.069	0.049
Secondary extinc. coeff. (mm)	0.56648×10^{-7}	0.15852×10^{-7}

TABLE 2
Positional Parameters and B_{eq} for $BiBa_2V_2PO_{11}$

Atom	Site	x	y	z	B_{eq}[a]
Bi	4e	0.50096(5)	−0.00090(7)	0.26613(5)	0.84(2)
Ba(1)	4e	0.73030(9)	−0.2321(1)	0.0569(1)	1.09(3)
Ba(2)	4e	0.94575(8)	0.2484(1)	0.11064(9)	0.96(3)
T(1)[b]	4e	0.5946(2)	0.2449(3)	0.0232(2)	0.61(8)
T(2)[b]	4e	0.8168(3)	0.0213(4)	0.3268(3)	0.7(1)
T(3)[b]	4e	0.1868(3)	−0.0240(4)	0.1707(3)	0.6(1)
O(1)	4e	0.874(1)	−0.452(2)	−0.038(1)	1.9(5)
O(2)	4e	0.888(1)	−0.048(2)	0.235(1)	1.4(4)
O(3)	4e	0.826(1)	−0.746(2)	0.329(2)	2.7(6)
O(4)	4e	0.686(1)	−0.056(2)	0.281(1)	2.2(6)
O(5)	4e	0.316(1)	0.050(2)	0.189(1)	1.7(5)
O(6)	4e	0.489(1)	−0.200(2)	0.121(1)	1.6(5)
O(7)	4e	0.514(1)	0.201(2)	0.130(1)	1.2(4)
O(8)	4e	0.871(1)	−0.453(2)	0.224(1)	1.8(5)
O(9)	4e	0.884(1)	−0.050(1)	−0.044(1)	1.1(4)
O(10)	4e	0.619(1)	−0.543(2)	0.028(1)	2.4(6)
O(11)	4e	0.709(1)	0.132(2)	0.051(1)	2.7(6)

[a] $B_{eq} = (8\pi^2/3)\Sigma_i\Sigma_j U_{ij} a^*_i a^*_j a_i a_j$.
[b] T = 2/3 V + 1/3 P.

ters at all three T sites showed that each was occupied with 1/3 P and 2/3 V. After refinement of the models with isotropic thermal parameters on each site, an empirical absorption correction using the program DIFABS (4) was applied. The data were also corrected for Lorentz and polarization effects. Final least-squares refinement on $|F|$ with anisotropic thermal parameters on each atom resulted in the final residuals $R = 0.055$ and $R_w = 0.069$. The final difference electron density map contains no features greater than 1.8% of a Bi atom. The refined atomic positional and isotropic thermal parameters are given in Table 2, and the anisotropic thermal parameters are given in Table 3. The results of refining isostructural $BiBa_2V_3O_{11}$ are given in Tables 1, 4, and 6. Selected bond distances and angles are given in Tables 5 and 6.

The results of the single crystal X-ray structure determinations were used to calculate the X-ray powder diffraction patterns using the program LAZY-PULVERIX (5). Tables 7 and 8 compare the calculated and the observed X-ray powder patterns for $BiBa_2V_2PO_{11}$ and $BiBa_2V_3O_{11}$, respectively.

The X-ray powder patterns of the indium and rare earth containing $MBa_2V_3O_{11}$ compounds (Table 9) were very similar to the patterns of $BiBa_2V_2PO_{11}$ and $BiBa_2V_3O_{11}$. In some cases, single crystals were grown and the isostructural nature was confirmed from single crystal X-ray data.

RESULTS AND DISCUSSION

The structures of $BiSr_2V_3O_{11}$ (I) and $BiBa_2V_3O_{11}$ (Fig. 2) are similar in that they both contain one pyrovanadate and one orthovanadate group per formula unit. Otherwise, these structures are very different. It is, of course, to be expected that the coordination of barium might be somewhat higher than that of strontium. However, the most significant difference between the two structures lies in the coordination of bismuth. In $BiSr_2V_3O_{11}$, a typical coordination of Bi^{III} is exhibited with the stereoactive lone pair of electrons. However, in $BiBa_2V_3O_{11}$, a stereoactive lone pair is not evident. This then accounts for

TABLE 3
Anisotropic Thermal Parameters (× 10^{-3} Å^2) for the Atoms of $BiBa_2V_2PO_{11}$

Atom	U_{33}	U_{22}	U_{11}	U_{32}	U_{31}	U_{21}
Bi	11.6(3)	8.7(3)	11.7(3)	0.4(2)	2.8(2)	0.6(2)
Ba(1)	14.2(5)	15.6(4)	11.5(5)	−0.6(4)	3.0(4)	−1.5(4)
Ba(2)	10.0(4)	16.7(5)	9.6(4)	−0.6(3)	1.7(3)	−0.3(4)
V(1)	6.0(1)	8.0(1)	9.0(1)	1.1(9)	2.0(1)	1.0(1)
V(2)	8.0(1)	9.0(1)	8.0(1)	−1.0(1)	1.0(1)	−1.0(1)
V(3)	6.0(1)	9.0(1)	7.0(1)	−1.0(1)	2.0(1)	−1.0(1)
O(1)	11.0(6)	27.0(7)	37.0(9)	3.0(5)	13.0(6)	15.0(6)
O(2)	11.0(6)	17.0(6)	25.0(7)	2.0(4)	3.0(5)	−4.0(5)
O(3)	50.0(1)	27.0(8)	31.0(9)	11.0(7)	12.0(8)	1.0(7)
O(4)	23.0(7)	37.0(8)	19.0(8)	2.0(6)	−1.0(6)	−6.0(6)
O(5)	35.0(8)	22.0(6)	12.0(7)	0.0(6)	15.0(6)	−2.0(5)
O(6)	4.0(5)	26.0(6)	29.0(8)	−8.0(5)	−1.0(5)	−6.0(6)
O(7)	11.0(6)	18.0(6)	19.0(7)	3.0(5)	5.0(5)	−2.0(5)
O(8)	19.0(7)	32.0(7)	23.0(7)	9.0(5)	18.(6)	10.(6)
O(9)	12.0(6)	15.0(5)	13.0(6)	−4.0(4)	0.0(5)	−2.0(5)
O(10)	50.0(1)	10.0(6)	34.0(9)	−10.0(6)	13.0(7)	−3.0(6)
O(11)	40.0(1)	24.0(7)	40.0(1)	−9.0(7)	10.0(8)	8.0(7)

TABLE 4
Positional Parameters and B_{eq} for $BiBa_2V_3O_{11}$

Atom	Site	x	y	z	B_{eq}[a]
Bi	4e	0.50111(7)	−0.0011(1)	0.26651(6)	0.71(1)
Ba(1)	4e	0.72755(7)	−0.2313(2)	0.05604(8)	1.10(2)
Ba(2)	4e	0.94492(6)	0.247(1)	0.11023(8)	0.93(2)
V(1)	4e	0.5977(2)	0.258(1)	0.0244(2)	0.61(4)
V(2)	4e	0.8185(6)	0.019(1)	0.3233(6)	0.7(2)
V(3)	4e	0.1853(6)	−0.020(1)	0.1674(7)	0.6(1)
O(1)	4e	0.873(2)	−0.445(3)	−0.035(2)	1.4(4)
O(2)	4e	0.894(2)	−0.054(3)	0.233(2)	1.4(4)
O(3)	4e	0.8329(9)	−0.750(2)	0.333(1)	1.7(2)
O(4)	4e	0.686(1)	−0.063(2)	0.279(2)	1.0(2)
O(5)	4e	0.319(2)	0.053(2)	0.188(2)	1.4(3)
O(6)	4e	0.489(1)	−0.196(2)	0.120(1)	0.9(2)
O(7)	4e	0.518(1)	0.200(2)	0.133(1)	1.1(2)
O(8)	4e	0.873(2)	−0.440(3)	0.219(2)	1.1(3)
O(9)	4e	0.890(2)	−0.060(3)	−0.039(2)	0.5(3)
O(10)	4e	0.626(1)	−0.544(2)	0.032(1)	1.9(3)
O(11)	4e	0.717(1)	0.132(2)	0.055(1)	1.2(2)

[a] $B_{eq} = (8\pi^2/3)\Sigma_i\Sigma_j U_{ij} a^*_i a^*_j a_i a_j$.

TABLE 5
Selected Interatomic Distances (Å) and Bond Angles (°) for $BiBa_2V_2PO_{11}$

Bi	–O(4)	2.27(1)	Ba(1)–O(1)	2.82(1)
	–O(5)	2.27(1)	–O(2)	2.82(1)
	–O(6)	2.21(1)	–O(4)	3.03(1)
	–O(6)	2.61(1)	–O(5)	3.04(1)
	–O(7)	2.20(1)	–O(6)	3.22(1)
	–O(7)	2.58(1)	–O(7)	3.25(1)
			–O(8)	2.80(1)
			–O(9)	2.79(1)
			–O(10)	2.72(1)
			–O(11)	2.79(1)
Ba(2)–O(1)		2.96(1)	V(1) –O(6)	1.75(1)
	–O(1)	2.85(1)	–O(7)	1.77(1)
	–O(2)	2.83(1)	–O(10)	1.64(1)
	–O(2)	2.82(1)	–O(11)	1.61(2)
	–O(3)	3.18(2)		
	–O(3)	3.15(2)	V(2) –O(1)	1.62(1)
	–O(8)	3.00(2)	–O(2)	1.60(1)
	–O(8)	2.86(1)	–O(3)	1.78(1)
	–O(9)	2.86(1)	–O(4)	1.68(1)
	–O(9)	2.81(1)		
	–O(11)	2.96(2)	V(3) –O(3)	1.70(1)
			–O(5)	1.64(1)
			–O(8)	1.61(1)
			–O(9)	1.60(1)
O(4)–Bi–O(5)		162.1(5)	O(4)–Bi–O(6)	79.9(5)
O(4)–Bi–O(6)		100.9(5)	O(4)–Bi–O(7)	87.1(5)
O(4)–Bi–O(7)		88.7(5)	O(5)–Bi–O(6)	86.5(5)
O(5)–Bi–O(6)		88.3(5)	O(5)–Bi–O(7)	80.7(5)
O(5)–Bi–O(7)		99.0(4)	O(6)–Bi–O(6)	161.8(4)
O(6)–Bi–O(7)		87.9(5)	O(6)–Bi–O(7)	74.5(4)
O(6)–Bi–O(7)		74.0(4)	O(6)–Bi–O(7)	123.5(4)
O(7)–Bi–O(7)		162.4(3)		
O(1)–Ba(1)–O(2)		100.2(4)	O(1)–Ba(1)–O(6)	146.4(4)
O(1)–Ba(1)–O(5)		85.5(3)	O(1)–Ba(1)–O(6)	145.3(4)
O(1)–Ba(1)–O(7)		111.0(4)	O(1)–Ba(1)–O(8)	63.8(4)
O(1)–Ba(1)–O(9)		66.1(4)	O(1)–Ba(1)–O(10)	77.2(4)
O(1)–Ba(1)–O(11)		130.1(4)	O(2)–Ba(1)–O(4)	53.9(4)
O(2)–Ba(1)–O(5)		112.1(3)	O(2)–Ba(1)–O(6)	108.6(3)
O(2)–Ba(1)–O(7)		143.7(3)	O(2)–Ba(1)–O(8)	66.7(4)
O(2)–Ba(1)–O(9)		68.0(3)	O(2)–Ba(1)–O(10)	139.8(4)
O(2)–Ba(1)–O(11)		64.4(4)	O(4)–Ba(1)–O(5)	122.1(4)
O(4)–Ba(1)–O(6)		54.8(3)	O(4)–Ba(1)–O(7)	101.2(3)
O(4)–Ba(1)–O(8)		84.6(4)	O(4)–Ba(1)–O(9)	113.1(4)
O(4)–Ba(1)–O(10)		107.8(4)	O(4)–Ba(1)–O(11)	62.9(4)
O(5)–Ba(1)–O(6)		100.7(3)	O(5)–Ba(1)–O(7)	54.7(3)
O(5)–Ba(1)–O(8)		147.6(3)	O(5)–Ba(1)–O(9)	53.1(3)
O(5)–Ba(1)–O(10)		107.7(4)	O(5)–Ba(1)–O(11)	61.7(4)
O(6)–Ba(1)–O(7)		52.0(3)	O(6)–Ba(1)–O(8)	110.4(3)
O(6)–Ba(1)–O(9)		143.1(3)	O(6)–Ba(1)–O(10)	68.4(4)
O(6)–Ba(1)–O(11)		81.0(4)	O(7)–Ba(1)–O(8)	144.3(4)
O(7)–Ba(1)–O(9)		107.8(3)	O(7)–Ba(1)–O(10)	67.9(4)
O(7)–Ba(1)–O(11)		81.0(4)	O(8)–Ba(1)–O(9)	101.8(4)
O(8)–Ba(1)–O(10)		76.8(5)	O(8)–Ba(1)–O(11)	130.9(5)
O(9)–Ba(1)–O(10)		138.7(4)	O(9)–Ba(1)–O(11)	64.2(4)
O(10)–Ba(1)–O(11)		145.5(5)		
O(1)–Ba(2)–O(1)		64.3(5)	O(1)–Ba(2)–O(2)	147.1(4)
O(1)–Ba(2)–O(2)		53.7(3)	O(1)–Ba(2)–O(3)	85.8(4)
O(1)–Ba(3)–O(3)		136.2(4)	O(1)–Ba(2)–O(8)	86.6(3)
O(1)–Ba(2)–O(8)		92.6(4)	O(1)–Ba(2)–O(9)	110.7(3)
O(1)–Ba(2)–O(9)		63.9(4)	O(1)–Ba(2)–O(11)	147.9(4)
O(1)–Ba(2)–O(2)		148.6(4)	O(1)–Ba(2)–O(2)	90.3(4)
O(1)–Ba(2)–O(3)		53.6(4)	O(1)–Ba(2)–O(3)	108.5(4)
O(1)–Ba(2)–O(8)		149.7(4)	O(1)–Ba(2)–O(8)	62.7(3)
O(1)–Ba(2)–O(9)		105.9(4)	O(1)–Ba(2)–O(9)	114.6(3)
O(1)–Ba(2)–O(11)		87.3(4)	O(2)–Ba(2)–O(2)	110.9(2)
O(2)–Ba(2)–O(3)		112.4(4)	O(2)–Ba(2)–O(3)	53.8(3)
O(2)–Ba(2)–O(8)		61.2(4)	O(2)–Ba(2)–O(8)	105.7(4)
O(2)–Ba(2)–O(9)		66.9(3)	O(2)–Ba(2)–O(9)	89.4(4)
O(2)–Ba(2)–O(11)		62.1(4)	O(2)–Ba(2)–O(3)	136.4(4)
O(2)–Ba(2)–O(3)		84.6(4)	O(2)–Ba(2)–O(8)	64.1(4)
O(2)–Ba(2)–O(8)		63.1(4)	O(2)–Ba(2)–O(9)	150.0(4)
O(2)–Ba(2)–O(9)		89.3(3)	O(2)–Ba(2)–O(11)	146.6(4)
O(3)–Ba(2)–O(3)		126.4(6)	O(3)–Ba(2)–O(8)	136.8(3)
O(3)–Ba(2)–O(8)		109.2(4)	O(3)–Ba(2)–O(9)	52.3(3)
O(3)–Ba(2)–O(9)		85.9(4)	O(3)–Ba(2)–O(11)	64.4(4)
O(3)–Ba(2)–O(8)		86.2(4)	O(3)–Ba(2)–O(8)	51.9(3)
O(3)–Ba(2)–O(9)		112.7(4)	O(3)–Ba(2)–O(9)	136.5(4)
O(3)–Ba(2)–O(11)		64.8(4)	O(8)–Ba(2)–O(8)	113.6(2)
O(8)–Ba(2)–O(9)		91.7(4)	O(8)–Ba(2)–O(9)	53.0(3)
O(8)–Ba(2)–O(11)		123.0(4)	O(8)–Ba(2)–O(9)	146.9(4)
O(8)–Ba(2)–O(9)		151.7(4)	O(8)–Ba(2)–O(11)	86.5(4)
O(9)–Ba(2)–O(9)		61.1(4)	O(9)–Ba(2)–O(11)	61.1(4)
O(9)–Ba(2)–O(11)		121.8(3)		
O(6)–V(1)–O(7)		107.7(6)	O(6)–V(1)–O(10)	106.5(7)
O(6)–V(1)–O(11)		111.7(7)	O(7)–V(1)–O(11)	107.1(7)
O(7)–V(1)–O(11)		111.6(7)	O(10)–V(1)–O(11)	111.9(8)
O(1)–V(2)–O(2)		108.7(7)	O(1)–V(2)–O(3)	107.5(8)
O(1)–V(2)–O(4)		110.9(7)	O(2)–V(2)–O(3)	107.2(7)
O(2)–V(2)–O(4)		108.3(7)	O(3)–V(2)–O(4)	114.0(8)
O(3)–V(3)–O(5)		115.3(8)	O(3)–V(3)–O(8)	105.9(8)
O(3)–V(3)–O(9)		108.8(8)	O(5)–V(3)–O(8)	111.3(7)
O(5)–V(3)–O(9)		107.6(7)	O(8)–V(3)–O(9)	107.8(7)

the fact that indium and rare earth cations readily substitute for Bi^{III} in $BiBa_2V_3O_{11}$ but not in $BiSr_2V_3O_{11}$. The distortion of the Bi^{III} octahedron in $BiBa_2V_3O_{11}$ is significant (Table 6), but this distortion can be largely attributed to the edge-sharing of the Bi–O octahedra. For the angles which would ideally be 90°, the largest deviation is the O(6)–Bi–O (7) angle (72.6°) and this could be mainly due to the Bi^{III}–Bi^{III} repulsion across the shared octahedral edge. Each Bi–O octahedron shares two edges, forming chains running along the *b* axis (Figs. 3, 4).

The difference in the structures of $BiBa_2V_3O_{11}$ and $BiSr_2V_3O_{11}$ may be partly due to the difference in sizes of barium and strontium. However, the major effect would seem to be related to covalency effects. The lone pair

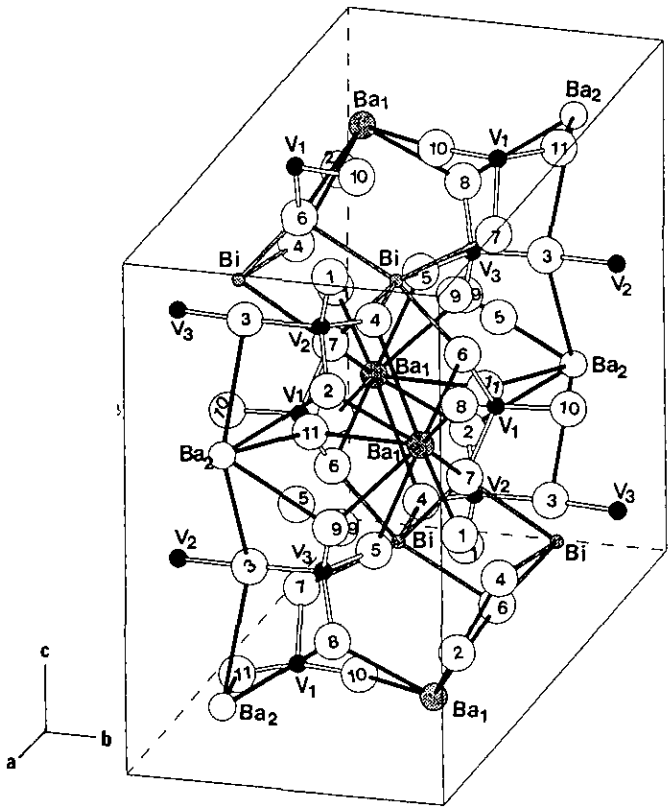

FIG. 2. Labeled sketch of the contents of a unit cell of $BiBa_2V_3O_{11}$. The big circles with only numbers represent oxygen atoms.

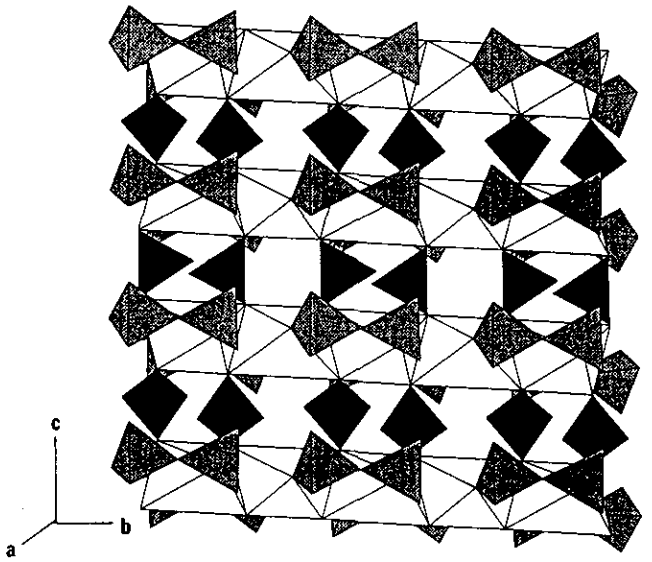

FIG. 4. The framework formed from BiO_4 chains, VO_4 groups, and V_2O_7 groups. The black shaded tetrahedra are VO_4 groups, the dot-matrix-filled tetrahedra are V_2O_7 groups, and the blank octahedra with solid edges are polyhedra of BiO_6.

influence on coordination tends to disappear as the covalency of the bonds increases. Thus, both forms of PbO show a pronounced lone pair effect in their structures, whereas PbS, PbSe, and PbTe have the simple sodium chloride structure with no lone pair distortion. Presumably as the 6*p* orbitals more strongly admix with ligand orbitals they are less available for the 6*s*–6*p* hybridization required for a lone pair distortion. On going from $BiSr_2V_3O_{11}$ to $BiBa_2V_3O_{11}$, the covalency of the Bi–O bonds increases through an inductive effect due to the higher ionicity of Ba–O vs Sr–O bonds. Analogous inductive effects in $Ba_2Bi^{III}Bi^{V}O_6$ (6) and $Na_2Bi_4^{III}Bi^{V}AuO_{11}$ (7) result in a fairly regular octahedron for Bi^{III} as well as for Bi^{V}.

Two crystallographically distinct Ba atoms are present in the $BiBa_2V_3O_{11}$ structure. The Ba(1) atom may be regarded as coordinated to 10 oxygen atoms (Fig. 5a), and the Ba(2) atom has 11 oxygen neighbor atoms (Fig. 5b). As expected, the average Ba–O bond length from 10-coordinated Ba(1) (2.927 Å in $BiBa_2V_3O_{11}$ and 2.928 Å in $BiBa_2V_2PO_{11}$) is slightly shorter than that of 11-coordinated Ba(2) (2.936 Å in $BiBa_2V_3O_{11}$ and 2.935 Å in $BiBa_2V_2PO_{11}$).

The V(1) atom is surrounded by four O atom neighbors forming a distorted tetrahedral orthovanadate group. The O–V–O angles are in the range 106.5 to 111.9° in $BiBa_2V_2PO_{11}$ and 104.4 to 113.0° in $BiBa_2V_3O_{11}$. The average T(1)–O bond length in $BiBa_2V_2PO_{11}$ (1.693 Å) is shorter than the V(1)–O distance in $BiBa_2V_3O_{11}$ (1.725 Å) which indicates mixing of V and P at the T(1) site. One of the V(1)–O distances in $BiBa_2V_3O_{11}$ is exceptionally short (1.57 Å) for a VO_4 tetrahedron, but this is readily rationalized because the O(10) atom involved is coordi-

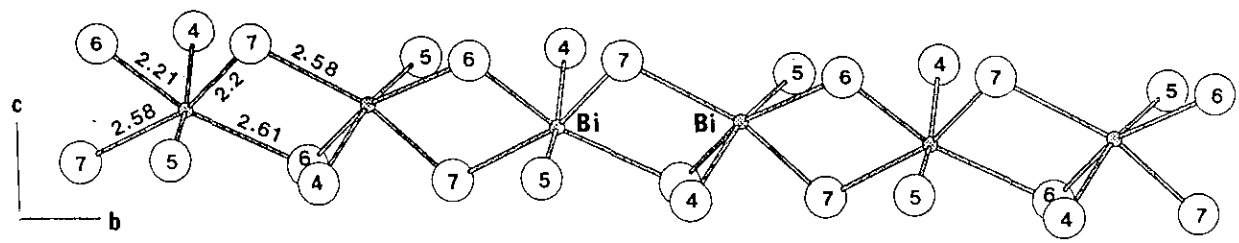

FIG. 3. Six coordinated Bi atoms in a BiO_4 chain.

TABLE 6
Selected Interatomic Distances (Å) and Bond Angles (°) for $BiBa_2V_3O_{11}$

Bi	–O(4)	2.30(2)	Ba(1)–O(1)	2.80(2)
	–O(5)	2.26(2)	–O(2)	2.87(2)
	–O(6)	2.21(1)	–O(4)	2.98(2)
	–O(6)	2.68(1)	–O(5)	3.01(2)
	–O(7)	2.21(1)	–O(6)	3.20(1)
	–O(7)	2.61(1)	–O(7)	3.28(1)
			–O(8)	2.78(2)
			–O(9)	2.81(2)
			–O(10)	2.72(2)
			–O(11)	2.82(1)
Ba(2)–O(1)		3.01(2)	V(1) –O(6)	1.80(1)
	–O(1)	2.92(3)	–O(7)	1.80(1)
	–O(2)	2.85(2)	–O(10)	1.57(2)
	–O(2)	2.80(2)	–O(11)	1.73(1)
	–O(3)	3.12(1)		
	–O(3)	3.13(1)	V(2) –O(1)	1.69(2)
	–O(8)	2.98(2)	–O(2)	1.64(2)
	–O(8)	2.95(2)	–O(3)	1.797(9)
	–O(9)	2.90(2)	–O(4)	1.72(2)
	–O(9)	2.76(2)		
	–O(11)	2.88(1)	V(3) –O(3)	1.795(9)
			–O(5)	1.71(2)
			–O(8)	1.71(1)
			–O(9)	1.65(2)
O(4)–Bi–O(5)		161.0(5)	O(4)–Bi–O(6)	78.7(5)
O(4)–Bi–O(6)		102.5(5)	O(4)–Bi–O(7)	86.8(5)
O(4)–Bi–O(7)		88.4(5)	O(5)–Bi–O(6)	86.6(6)
O(5)–Bi–O(6)		87.5(5)	O(5)–Bi–O(7)	80.7(6)
O(5)–Bi–O(7)		99.1(4)	O(6)–Bi–O(6)	160.9(4)
O(6)–Bi–O(7)		88.5(5)	O(6)–Bi–O(7)	73.8(4)
O(6)–Bi–O(7)		72.6(4)	O(6)–Bi–O(7)	125.1(4)
O(7)–Bi–O(7)		162.3(3)		
O(1)–Ba(1)–O(2)		96.9(6)	O(1)–Ba(1)–O(6)	144.6(5)
O(1)–Ba(1)–O(5)		86.6(6)	O(1)–Ba(1)–O(6)	146.3(5)
O(1)–Ba(1)–O(7)		112.2(5)	O(1)–Ba(1)–O(8)	61.8(6)
O(1)–Ba(1)–O(9)		64.5(4)	O(1)–Ba(1)–O(10)	75.9(6)
O(1)–Ba(1)–O(11)		128.5(6)	O(2)–Ba(1)–O(4)	55.7(5)
O(2)–Ba(1)–O(5)		111.9(6)	O(2)–Ba(1)–O(6)	110.6(5)
O(2)–Ba(1)–O(7)		145.4(5)	O(2)–Ba(1)–O(8)	64.3(4)
O(2)–Ba(1)–O(9)		65.2(6)	O(2)–Ba(1)–O(10)	137.5(6)
O(2)–Ba(1)–O(11)		63.3(5)	O(4)–Ba(1)–O(5)	122.5(4)
O(4)–Ba(1)–O(6)		55.0(4)	O(4)–Ba(1)–O(7)	101.8(4)
O(4)–Ba(1)–O(8)		84.5(5)	O(4)–Ba(1)–O(9)	113.0(5)
O(4)–Ba(1)–O(10)		108.0(5)	O(4)–Ba(1)–O(11)	63.3(4)
O(5)–Ba(1)–O(6)		100.1(4)	O(5)–Ba(1)–O(7)	54.6(4)
O(5)–Ba(1)–O(8)		146.3(5)	O(5)–Ba(1)–O(9)	55.7(5)
O(5)–Ba(1)–O(10)		109.4(5)	O(5)–Ba(1)–O(11)	62.5(5)
O(6)–Ba(1)–O(7)		51.9(3)	O(6)–Ba(1)–O(8)	112.7(5)
O(6)–Ba(1)–O(9)		144.9(5)	O(6)–Ba(1)–O(10)	70.7(4)
O(6)–Ba(1)–O(11)		82.6(4)	O(7)–Ba(1)–O(8)	146.2(5)
O(7)–Ba(1)–O(9)		110.3(4)	O(7)–Ba(1)–O(10)	70.5(4)
O(7)–Ba(1)–O(11)		83.5(4)	O(8)–Ba(1)–O(9)	97.0(6)
O(8)–Ba(1)–O(10)		76.0(6)	O(8)–Ba(1)–O(11)	127.5(5)
O(9)–Ba(1)–O(10)		137.6(5)	O(9)–Ba(1)–O(11)	64.1(5)
O(10)–Ba(1)–O(11)		150.6(5)		
O(1)–Ba(2)–O(1)		64.8(7)	O(1)–Ba(2)–O(2)	144.8(6)
O(1)–Ba(2)–O(2)		55.2(6)	O(1)–Ba(2)–O(3)	84.2(5)
O(1)–Ba(3)–O(3)		136.0(5)	O(1)–Ba(2)–O(8)	85.9(6)
O(1)–Ba(2)–O(8)		90.8(7)	O(1)–Ba(2)–O(9)	110.2(7)
O(1)–Ba(2)–O(9)		62.4(3)	O(1)–Ba(2)–O(11)	148.6(5)
O(1)–Ba(2)–O(2)		150.3(6)	O(1)–Ba(2)–O(2)	89.1(7)
O(1)–Ba(2)–O(3)		54.7(5)	O(1)–Ba(2)–O(3)	107.9(5)
O(1)–Ba(2)–O(8)		148.0(6)	O(1)–Ba(2)–O(8)	58.5(6)
O(1)–Ba(2)–O(9)		110.1(3)	O(1)–Ba(2)–O(9)	114.7(7)
O(1)–Ba(2)–O(11)		88.4(5)	O(2)–Ba(2)–O(2)	110.2(3)
O(2)–Ba(2)–O(3)		113.5(5)	O(2)–Ba(2)–O(3)	55.4(4)
O(2)–Ba(2)–O(8)		60.4(6)	O(2)–Ba(2)–O(8)	110.4(3)
O(2)–Ba(2)–O(9)		64.2(6)	O(2)–Ba(2)–O(9)	88.3(6)
O(2)–Ba(2)–O(11)		62.7(5)	O(2)–Ba(2)–O(3)	135.8(4)
O(2)–Ba(2)–O(3)		82.4(5)	O(2)–Ba(2)–O(8)	62.5(4)
O(2)–Ba(2)–O(8)		61.4(6)	O(2)–Ba(2)–O(9)	148.9(6)
O(2)–Ba(2)–O(9)		90.5(6)	O(2)–Ba(2)–O(11)	145.4(5)
O(3)–Ba(2)–O(3)		129.0(4)	O(3)–Ba(2)–O(8)	138.4(5)
O(3)–Ba(2)–O(8)		107.8(4)	O(3)–Ba(2)–O(9)	55.4(4)
O(3)–Ba(2)–O(9)		84.3(4)	O(3)–Ba(2)–O(11)	66.3(3)
O(3)–Ba(2)–O(8)		83.9(4)	O(3)–Ba(2)–O(8)	55.1(4)
O(3)–Ba(2)–O(9)		112.7(4)	O(3)–Ba(2)–O(9)	136.6(5)
O(3)–Ba(2)–O(11)		65.7(3)	O(8)–Ba(2)–O(8)	112.7(3)
O(8)–Ba(2)–O(9)		91.1(6)	O(8)–Ba(2)–O(9)	55.5(5)
O(8)–Ba(2)–O(11)		123.1(5)	O(8)–Ba(2)–O(9)	149.6(5)
O(8)–Ba(2)–O(9)		149.9(6)	O(8)–Ba(2)–O(11)	88.3(5)
O(9)–Ba(2)–O(9)		59.5(7)	O(9)–Ba(2)–O(11)	62.2(5)
O(9)–Ba(2)–O(11)		121.6(5)		
O(6)–V(1)–O(7)		104.4(6)	O(6)–V(1)–O(10)	113.0(8)
O(6)–V(1)–O(11)		109.1(7)	O(7)–V(1)–O(10)	110.6(8)
O(7)–V(1)–O(11)		107.4(7)	O(10)–V(1)–O(11)	112.0(8)
O(1)–V(2)–O(2)		108(1)	O(1)–V(2)–O(3)	106(1)
O(1)–V(2)–O(4)		107(1)	O(2)–V(2)–O(3)	109(1)
O(2)–V(2)–O(4)		109(1)	O(3)–V(2)–O(4)	117.5(8)
O(3)–V(3)–O(5)		116.6(8)	O(3)–V(3)–O(8)	106.7(9)
O(3)–V(3)–O(9)		109.0(9)	O(5)–V(3)–O(8)	109(1)
O(5)–V(3)–O(9)		109(1)	O(8)–V(3)–O(9)	106(1)

nated to only V(1) and Ba(1), whereas all other oxygens have a coordination number of 3 or 4. The thermal parameter for O(10) is also relatively high (Table 4), as might be expected for such a low coordination number.

The pyrovanadate group in $BiBa_2V_3O_{11}$ is formed from the VO_4 tetrahedra of V(2) and V(3) atoms through the bridging atom O(3) (Fig. 6). The V–O bond lengths for the bridging O atom [V(2)–O(3), 1.797 Å; V(3)–O(3), 1.795 Å] are longer than those for the other six terminal oxygen atoms (average bond length 1.687 Å), and such a trend was observed in other compounds containing a pyrovanadate group (1, 8–11). The V(2)–O(3)–V(3) angle in $BiBa_2V_3O_{11}$ (167°) is much larger than that observed in $BiSr_2V_3O_{11}$ [125°] (1), α–$Sr_2V_2O_7$ [121 and 123°] (12), and

TABLE 7
Indexed X-ray Powder Pattern for $BiBa_2V_2PO_{11}$

	Calcd.		Obsd.	
h k l	*d*	*I*	*d*	*I*
1 0 0	11.937	53	11.952	43
1 1 0	6.420	5	6.398	3
2 0 0	5.968	17	5.968	17
0 0 2	5.504	9	5.501	17
1 0 −2	5.503	9		
2 1 0	4.697	7	4.685	14
1 0 2	4.611	23	4.612	40
2 0 −2	4.610	23		
0 1 2	4.461	4	4.454	6
1 1 −2	4.461	3		
3 0 0	3.979	22	3.980	18
1 1 2	3.944	29	3.939	45
2 1 −2	3.944	28		
2 0 2	3.649	23	3.648	49
3 0 −2	3.648	24		
1 2 0	3.627	31	3.627	
3 1 0	3.526	56	3.523	65
2 1 2	3.291	35	3.288	55
3 1 −2	3.290	35		
2 2 0	3.210	8	3.200	8
0 2 2	3.131	100	3.128	100
1 2 −2	3.131	98		
4 0 0	2.984	16	2.984	17
3 0 2	2.921	34	2.922	62
4 0 −2	2.920	33		
1 0 −4	2.828	73	2.829	51
3 2 0	2.751	55	2.746	41
2 2 2	2.634	12	2.629	14
3 2 −2	2.634	12		
0 3 1	2.473	4	2.465	4
1 1 4	2.423	4	2.421	6
3 1 −4	2.423	4		
5 0 0	2.387	10	2.388	14
3 2 2	2.317	5	2.316	7
4 2 −2	2.317	6		
0 2 4	2.230	22	2.228	28
2 2 −4	2.230	23		
1 3 2	2.224	11	2.219	15
2 3 −2	2.224	11		
2 1 4	2.206	17	2.207	23
4 1 −4	2.206	17		
3 3 0	2.140	20	2.135	15
3 0 4	2.053	8	2.053	14
5 0 −4	2.053	9		
4 2 2	2.031	25	2.029	47
5 2 −2	2.031	26		
5 0 2	2.026	14		
6 0 −2	2.026	15		
2 2 4	1.972	18	1.969	19
4 2 −4	1.972	18		
0 4 0	1.904	27	1.896	16
6 2 0	1.763	21	1.762	18
6 0 2	1.747	7	1.747	13
7 0 −2	1.747	7		
1 2 −6	1.685	13	1.684	14
6 2 −2	1.685	12		
3 4 2	1.595	11	1.590	17
4 4 −2	1.595	11		
1 4 −4	1.579	22	1.575	10

TABLE 8
Indexed X-ray Powder Pattern for $BiBa_2V_3O_{11}$

	Calcd.		Obsd.	
h k l	*d*	*I*	*d*	*I*
1 0 0	12.005	47	12.090	31
1 1 0	6.511	4	6.507	4
2 0 0	6.003	15	6.017	27
0 0 2	5.490	8	5.497	9
1 0 −2	5.490	8		
2 1 0	4.746	6	4.751	10
1 0 2	4.610	19	4.619	29
2 0 −2	4.610	18		
0 1 2	4.480	4	4.489	6
1 1 −2	4.480	4		
3 0 0	4.002	20	4.007	30
1 1 2	3.962	24	3.968	30
2 1 −2	3.962	24		
2 0 2	3.656	24	3.660	55
3 0 −2	3.656	24		
3 1 0	3.556	54	3.557	60
2 1 2	3.307	31	3.307	54
3 1 −2	3.307	31		
2 2 0	3.210	6	3.198	11
0 2 2	3.166	100	3.166	100
1 2 −2	3.166	97		
4 0 0	3.001	13	3.001	25
3 0 2	2.931	34	2.930	78
4 0 −2	2.931	34		
1 0 −4	2.820	70	2.821	60
3 2 0	2.784	57	2.783	49
2 2 2	2.659	12	2.659	16
3 2 −2	2.659	12		
0 3 1	2.515	3	2.512	3
1 1 4	2.424	5	2.423	6
3 1 −4	2.423	4		
5 0 0	2.401	10	2.401	16
3 2 2	2.337	5	2.335	5
4 2 −2	2.337	5	2.335	5
1 3 2	2.254	10	2.252	15
2 3 −2	2.254	10		
0 2 4	2.240	18	2.239	21
2 2 −4	2.240	19		
2 1 4	2.209	16	2.207	22
4 1 −4	2.209	17		
3 3 0	2.170	21	2.167	18
3 0 4	2.055	7	2.053	8
5 0 −4	2.055	7	2.052	8
4 2 2	2.048	22	2.045	18
5 2 −2	2.048	21	2.044	18
5 0 2	2.036	13	2.034	23
6 0 −2	2.036	13	2.034	23
2 2 4	1.981	19	1.978	19
4 2 −4	1.981	19		
0 4 0	1.938	26	1.934	32
6 2 0	1.778	21	1.774	25
6 0 2	1.755	7	1.752	12
7 0 −2	1.755	7	1.752	12
1 2 −6	1.687	13	1.684	13
6 2 −2	1.687	12		
3 4 2	1.616	12	1.612	13
4 4 −2	1.616	12		
1 4 −4	1.597	23	1.593	18

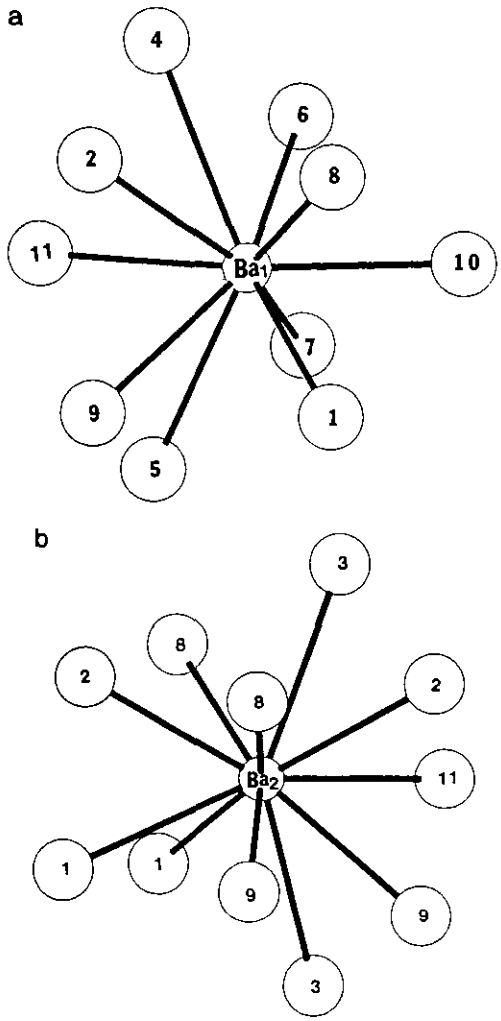

FIG. 5. Coordination polyhedron of Ba(1) and Ba(2) atoms.

β–$Sr_2V_2O_7$ [123 and 124°] (11). The V_2O_7 group is grafted onto the BiO_4 chains by sharing the nonbridging oxygens of the Bi–O octahedra, the V–V axis being in essentially the same orientation as the BiO_4 chains (Fig. 4). Each V_2O_7 group is thus bound to two different Bi–O octahedra, which stretches the V–O–V angle to a value somewhat higher than usual. Because of the partial replacement of V by P atoms in $BiBa_2V_2PO_{11}$, the T–O bond

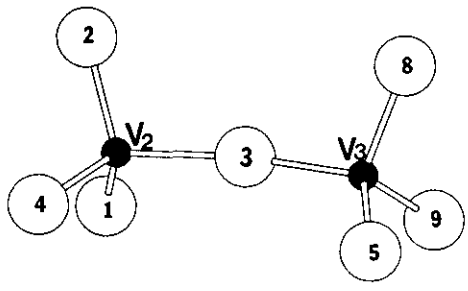

FIG. 6. Pyrovanadate group V_2O_7.

TABLE 9
Cell Parameters for $MBa_2V_3O_{11}$

M	a	b	c	β
Bi	12.332(3)	7.750(4)	11.279(6)	103.2(2)
In	12.077(6)	7.528(9)	10.985(8)	104.1(5)
Sc	12.035(8)	7.552(9)	11.029(6)	103.6(5)
Y	12.305(7)	7.739(4)	11.277(6)	103.1(5)
La	12.645(6)	7.820(4)	11.516(8)	104.9(6)
Ce	12.34(1)	7.759(6)	11.256(9)	103.1(5)
Pr	12.429(8)	7.767(5)	11.250(9)	103.3(5)
Nd	12.371(8)	7.759(6)	11.258(9)	103.5(5)
Sm	12.348(7)	7.739(6)	11.235(9)	103.0(5)
Eu	12.362(6)	7.747(5)	11.275(9)	103.4(5)
Gd	12.340(9)	7.742(6)	11.249(8)	103.3(4)
Tb	12.352(7)	7.733(6)	11.275(9)	103.4(5)
Dy	12.300(8)	7.700(6)	11.248(9)	103.1(5)
Ho	12.326(7)	7.739(6)	11.254(9)	103.1(5)
Er	12.34(1)	7.805(6)	11.528(9)	104.4(5)
Yb	12.33(1)	7.729(6)	11.304(9)	103.1(5)
Lu	12.502(7)	7.617(6)	11.285(9)	102.7(5)

lengths of the T_2O_7 group are also much shorter than those in $BiBa_2V_3O_{11}$ (Tables 5 and 6).

When the V of $BiBa_2V_3O_{11}$ is partially replaced with P to produce $BiBa_2V_2PO_{11}$, the cell volume decreases as expected. However, as the a and b axes decrease in length, the c axis actually increases despite a nearly constant β angle. We may rationalize this as a compression along the a and b axes which causes the structure to squeeze out in the c direction. An analogous effect has been noted in the cordierite structure (13).

ACKNOWLEDGMENT

This work was supported by the Oregon Metals Initiative, which is funded through partnership with the Oregon Economic Development Department and Oregon Lottery, the U.S. Bureau of Mines, Teledyne Wah Chang Albany, and Pacific Power and Light.

REFERENCES

1. J. Huang and A. Sleight, *J. Solid State Chem.* **97,** 228 (1992).
2. Molecular Structure Corporation, "TEXSAN," The Woodlands, TX (1989).
3. G. M. Sheldrick, C. Kruger, and R. Goddard (Eds.), "Crystallographic Computing 3," pp. 175–189. Oxford Univ. Press, 1985.
4. N. Walker and D. Stuart, *Acta Crystallogr.* **A39,** 158 (1983).
5. K. Yvon, W. Jeitschko, and E. Parthe, *J. Appl. Crystallogr.* **10,** 73 (1977).
6. D. E. Cox and A. W. Sleight, *Solid State Commun.* **19,** 969 (1976).
7. J. Pannetier, D. Tranqui, and A. W. Sleight, *Mater. Res. Bull.* **28,** 989 (1993).
8. E. E. Sauerbrei, R. Faggiani, and C. Calvo, *Acta Crystallogr.* **B30,** 2907 (1974).
9. R. Gopal, and C. Calvo, *Acta Crystallogr.* **B30,** 2491 (1974).
10. M. Quarton, J. Angenault, and A. Rimsky, *Acta Crystallogr.* **B29,** 567 (1973).
11. J. A. Baglio, and J. N. Dann, *J. Solid State Chem.* **4,** 87 (1972).
12. J. Huang and A. W. Sleight, *Mater. Res. Bull.* 27, 581 (1992).
13. U. Chowdhry and A. W. Sleight, *Annu. Rev. Mater. Sci.* **17,** 323 (1987).